1521-0103/369/3/406–418$35.00
THE JOURNAL OF PHARMACOLOGY AND EXPERIMENTAL THERAPEUTICS

https://doi.org/10.1124/jpet.118.255562
J Pharmacol Exp Ther 369:406–418, June 2019

Exposure-Effect Relationships in Established Rat Adjuvant-Induced and Collagen-Induced Arthritis: A Translational Pharmacokinetic-Pharmacodynamic Analysis[S]

Harvey Wong, Lichuan Liu, Wenjun Ouyang, Yuzhong Deng, Matthew R. Wright, and Cornelis E.C.A. Hop

Departments of Drug Metabolism and Pharmacokinetics (H.W., L.L., Y.D., M.R.W., C.E.C.A.H.) and Immunology (W.O.), Genentech Inc., South San Francisco, California

Received December 2, 2018; accepted April 1, 2019

ABSTRACT

The ability of rodent immune-mediated arthritis models to quantitatively predict therapeutic activity of antiarthritis agents is poorly understood. Two commonly used preclinical models of arthritis are adjuvant-induced arthritis (AIA) and collagen-induced arthritis (CIA) in rats. The objective of the current study is to investigate the relationship between efficacy in AIA and CIA in rats, and clinical efficacy in rheumatoid arthritis patients using translational pharmacokinetic-pharmacodynamic (PK-PD) analysis. A range of doses of indomethacin (a nonsteroidal anti-inflammatory drug), and three disease-modifying antirheumatic drugs (DMARDs), methotrexate, etanercept, and tofacitinib, were evaluated in AIA and CIA rats. Dexamethasone was included in this study as a positive control. The area under the ankle diameter-time profile (AUC_{ankle}) and ankle histopathology summed scores (AHSS) were used as efficacy endpoints for activity against disease symptoms (joint inflammation) and disease progression (joint damage), respectively. Translational PK-PD analysis was performed to rank order preclinical efficacy endpoints at clinically relevant concentrations. For each drug tested, inhibition of AUC_{ankle} and AHSS scores was generally comparable in both magnitude and rank order. Overall, based on both AUC_{ankle} and the AHSS inhibition, the rank ordering of preclinical activity for the DMARDs evaluated was tofacitinib $>$ etanercept $\geq$ methotrexate. This ranking of preclinical efficacy was consistent with reported clinical efficacy. Of interest, indomethacin showed equal or often better efficacy than the three DMARDs evaluated on inhibiting AHSS despite having limited ability to prevent joint damage clinically in patients. The translational value of performing PK-PD analysis of arthritis models in rats is discussed.

Introduction

High attrition rates plague the drug discovery and development process with phase II clinical trial success rates being <20% (Arrowsmith and Miller, 2013). By far, the most prominent reason for failure is lack of efficacy (>50% for both phases II and III), highlighting a need to improve the predictability of preclinical disease models used in the identification of drug candidates. Rheumatoid arthritis (RA) is a chronic debilitating autoimmune disorder causing inflammation of many joints including those of the hands and feet. Finding treatments for RA remains a challenge since it is heterogeneous in nature and the biologic mechanisms causing the disease are not well understood (Kollias et al., 2011). Rodent models of immune-mediated arthritis remain a common and valuable approach for evaluation of mechanisms of inflammatory joint disease and relative efficacy of antiarthritic agents (Kannan et al., 2005; Hegen et al., 2008; Bolon et al., 2011; Caplazi et al., 2015). Qualitatively, these models have characteristics that display both similarities and differences in patients with RA. Two of the most commonly used rodent models used to evaluate existing or investigative therapies for rheumatoid arthritis are adjuvant-induced arthritis (AIA) and collagen-induced arthritis (CIA) in rats (Hegen et al., 2008; Bolon et al., 2011).

The first model of rheumatoid arthritis described was AIA in rats (Pearson, 1956). AIA is induced by a single injection of complete Freund adjuvant in Lewis rats and characterized by rapid disease onset, severe polyarticular inflammation, bone resorption, and perosteal bone proliferation. Disease progression onset occurs 10 days after adjuvant injection and usually lasts less than 1 month. AIA in rats is a T-cell and neutrophil-dependent disease that is complement independent, and has no documented role for B-cells (Hegen et al., 2008). Similar to human disease, AIA results in swelling and loss of function of joints, cartilage damage, and lymphocyte infiltration. However, bone resorption is more prominent in AIA rats compared

https://doi.org/10.1124/jpet.118.255562.
[S] This article has supplemental material available at jpet.aspetjournals.org.

ABBREVIATIONS: AD, ankle diameter; AHSS, ankle histopathology summed score; AIA, adjuvant-induced arthritis; AUC_{ankle}, area under the ankle diameter-time profile; C, concentration; CIA, collagen-induced arthritis; C_{ss}, steady-state concentration; DMARD, disease-modifying antirheumatic drug; E_{max}, maximum percentage of inhibition of the ankle histopathology score; I_{AS}, rate constant describing the reduction of ankle swelling by the drugs used in the adjuvant-induced and collagen-induced arthritis studies; %inh_score, percentage of inhibition of the ankle histopathology score; k_{in}, rate of increase in ankle diameter; PK-PD, pharmacokinetic-pharmacodynamic; RA, rheumatoid arthritis; TNF, tumor necrosis factor.

with both CIA rats and human RA. In addition, unlike human RA, the gastrointestinal and genitourinary tracts, skin, and eyes are affected in AIA. CIA in rats was first described by Trentham et al. (1977) and has similarity to human RA in that females are more susceptible to arthritis in this model. Arthritis onset is rapid, usually developing 10–13 days after immunization with homologous or heterologous type II collagen, peaking at about days 15–20 and then gradually declining. The resulting polyarthritis is characterized by marked cartilage destruction associated with immune complex deposition on articular surfaces, bone resorption, periosteal proliferation, and moderate to marked synovitis and periarticular inflammation (Bendele, 2001). Collagen-specific T- and B-cells are both required for disease induction, and CIA can be transferred with serum from diseased animals into recipient strains. Rat CIA differs from human RA in that it is self-limiting and not characterized by exacerbations and remissions. Furthermore, the inflammatory cell infiltrate in rat CIA consists predominantly of polymorphonuclear cells, whereas a high proportion of mononuclear cells are seen in human RA (Hegen et al., 2008). CIA in rats differs from AIA in that it is less severe and complement dependent, with no involvement of B-cells. Despite the broad use of AIA and CIA rats in the evaluation of new RA therapies, there has been no detailed characterization of drug concentration-effect relationships limiting the understanding of the translatability of findings in these preclinical models to humans.

Preclinical pharmacokinetic-pharmacodynamic (PK-PD) analysis can play an important role in the drug discovery and development process by providing an integrated assessment of the relationships between drug concentrations in the body and efficacy (Liu et al., 2011; Wong et al., 2012a,b, 2017; Schuck et al., 2015). In particular, PK-PD analysis allows for the quantitative translation of species differences in pharmacokinetics and/or in vivo drug potency. The primary objective of the current study was to perform a detailed PK-PD analysis of the effect of drugs commonly used to treat RA in therapeutic AIA and CIA rats. The PK-PD analysis will provide detailed understanding of drug concentration-effect relationships and facilitate translation of preclinical efficacy in therapeutic AIA and CIA rats to clinical efficacy. Such information is currently lacking, making it difficult to understand how the performance of new drug candidates in these efficacy models will translate to clinical efficacy in rheumatoid arthritis patients. The four drugs tested were indomethacin (a nonsteroidal anti-inflammatory drug), methotrexate [a standard-of-care disease-modifying antirheumatic drug (DMARD)], etanercept [an anti-tumor necrosis factor (TNF) biologic], and tofacitinib (a recently approved oral Janus kinase inhibitor). Dexamethasone (a corticosteroid), which is delivered by local injection in humans, was included since it serves as a common positive control in both preclinical models.

Materials and Methods

Adjuvant-Induced Arthritis

Efficacy. Male Lewis rats (Charles River Laboratories, Wilmington, MA) weighing 204–262 g (average weight = 230 g) were used for AIA studies. Rats (n = 8 per group for arthritis efficacy groups; n = 4 per group for normal control rats; and n = 3 per group for supporting pharmacokinetic satellite groups) were anesthetized with isoflurane and injected with 100 μl of Freund's Complete Adjuvant (Sigma-Aldrich, St. Louis, MO) containing lipoidal amine (60 mg/ml; Bolder BioPATH, Inc., Boulder, CO) at the base of the tail on day 0. On study days 8 to 9, onset of arthritis occurred. Ankle caliper measurements were made with a Digitrix II micrometer (Fowler & NSK). On study day 9 (day 1 of established disease), rats were randomized into treatment groups with each group having balanced mean ankle diameters. Randomization was performed after ankle joint swelling was established and there was good evidence of bilateral disease. Rats with outlier ankle measurements (i.e., low or high scores) were kept for supporting pharmacokinetic satellite groups. Dosing was initiated upon enrollment (day 1 of established disease). The doses and dosing regimens of various test agents are indicated in Table 1. Animals in the main efficacy groups were euthanized following end of study on day 8 of established disease. The area under the ankle diameter-time profile (AUC_{ankle}) for each treatment group was determined using the trapezoid rule (Gibaldi and Perrier, 1982). The percentage of inhibition of AUC_{ankle} was determined using eq. 4, as described subsequently in *PK-PD Analysis of Ankle Swelling*. This basic study design and animal usage was approved by Bolder BioPATH's Institutional Animal Care and Use Committee for compliance with regulations prior to study initiation.

Pharmacokinetics. Supporting pharmacokinetic information in the AIA studies was gathered at doses (n = 3 rats per group) covering the range of doses used for each agent (see Table 1). AIA rats in the pharmacokinetic satellite groups were dosed similarly to the main efficacy groups and whenever possible pharmacokinetic assessments were taken on the last day of study (day 7 of established disease). The pharmacokinetic assessment in the high-dose groups for indomethacin (6 mg/kg) was taken following the first dose on day 1 of established disease due to potential tolerability concerns at these doses. Etanercept pharmacokinetic assessments were made on both days 1 and 7 of established disease to assess any potential changes in etanercept exposure following multiple doses resulting from antitherapeutic antibodies. On the day of the pharmacokinetic assessment, plasma (indomethacin, methotrexate, tofacitinib, and dexamethasone) or serum (etanercept) samples were taken at 0.25, 0.5, 1, 3, 6, 9, 12, and 24 hours postdose. Plasma/serum samples were stored frozen until concentrations were assessed. The concentrations of indomethacin (Sigma-Aldrich), methotrexate (Sigma-Aldrich), tofacitinib (Genentech, South San Francisco, CA), and dexamethasone (Vedco Inc., Saint Joseph, MO) in plasma were determined by liquid chromatography–tandem mass spectrometry. Etanercept (Amgen, Thousand Oaks, CA) serum concentrations were determined by enzyme-linked immunosorbent assays. Rats used for pharmacokinetic assessment were euthanized after the final 24-hour sampling on day 1 or 7. The estimated pharmacokinetic parameters for AIA rats are given in Supplemental Table 6.

Ankle Histopathology. Preserved and decalcified (5% formic acid) ankle joints were cut in the sagittal plane into two approximately equal halves and processed for paraffin embedding, sectioned, and stained with toluidine blue. Tissues were examined microscopically, and adjuvant arthritic ankles were given scores of 0–7 for inflammation, bone resorption, cartilage damage, and pannus, where a score of 0 represents normal with increasing numbers representing increasing severity of disease. A detailed description of the criteria for the scores is given in Supplemental Table 1. Summed inflammation, pannus, bone, and cartilage scores were derived and group mean values were compared using one-way ANOVA with significance set at $P < 0.05$.

Collagen-Induced Arthritis

Efficacy. Female Lewis rats (Charles River Laboratories) weighing 156–189 g (average weight = 172 g) were used for CIA studies. Rats (n = 8 per group for arthritis efficacy groups; n = 4 per group for normal control rats; and n = 3 per group for supporting pharmacokinetic satellite groups) were anesthetized with isoflurane and injected with 300 μl of Freund's Incomplete Adjuvant (Difco, Detroit, MI) containing 2 mg/ml bovine type II collagen (Elastin Products, Owensville, MO) at

TABLE 1
Study design information for antiarthritis agents tested in AIA and CIA rats

Drug	Efficacy: Dose and Regimen	Supporting Pharmacokinetics: Doses and Assessment Times
Indomethacin	Vehicle (CMC), 0.1, 0.3, 1, 3, or 6 mg/kg indomethacin was given by mouth daily on days 1–7 of established disease.	Doses of 0.1, 1, and 6 mg/kg indomethacin were given by mouth on day 1 (6 mg/kg) or day 7 (0.1 and 1 mg/kg) of established disease.
Methotrexate	Vehicle (CMC), 0.1, 0.3, or 1 mg/kg methotrexate was given by mouth daily on days 1–7 of established disease.	Doses of 0.1 and 1 mg/kg methotrexate were given by mouth on day 7 of established disease.
Etanercept	Vehicle (sterile water), 0.3, 1, 3, 10, or 30 mg/kg etanercept was given via subcutaneous injection every third day on days 1, 4, and 7 of established disease.	Doses of 0.3, 1, 3, 10, and 30 mg/kg, s.c., were given on days 1 and 7 of established disease.
Tofacitinib	Vehicle (MCT), 0.5, 1.5, 5, 15, or 45 mg/kg tofacitinib was given by mouth daily on days 1–7 of established disease.	Doses of 0.5, 5, and 45 mg/kg tofacitinib were given by mouth on day 7 of established disease.
Dexamethasone	Vehicle (CMC), 0.0125, 0.025, 0.05, 0.1, or 0.2 mg/kg dexamethasone was given by mouth daily on days 1–7 of established disease.	Doses of 0.0125, 0.05, and 0.2 mg/kg dexamethasone were given by mouth on day 7 of established disease.

CMC, 1% carboxymethylcellulose; MCT, 0.5% methylcellulose with 0.2% Tween 80.

the base of the tail and at two sites on the back on days 0 and 6. Ankle caliper measurements were made with a Digitrix II micrometer (Fowler & NSK). By study day 10 (day 1 of established disease), onset of arthritis occurred and rats were randomized into treatment groups with each group having balanced mean ankle diameters. Randomization was performed after ankle joint swelling was established and there was good evidence of bilateral disease. Rats with outlier ankle measurements (i.e., low or high scores) were kept for supporting pharmacokinetic satellite groups (as detailed subsequently). Dosing was initiated upon enrollment (day 1 of established disease). The doses and dosing regimens of various test agents are indicated in Table 1. Animals in the main efficacy groups were euthanized following the end of study on day 8 of established disease. The AUC_{ankle} and percentage of inhibition of AUC_{ankle} values were as described previously for the AIA model. This basic study design and animal usage were approved by Bolder BioPATH's Institutional Animal Care and Use Committee for compliance with regulations prior to study initiation.

Pharmacokinetics. The supporting pharmacokinetics for CIA studies were evaluated in a similar manner as described previously for the AIA studies. The estimated pharmacokinetic parameters for CIA rats are given in Supplemental Table 6.

Ankle Histopathology. Preserved and decalcified (5% formic acid) ankle joints were cut in half longitudinally, processed through graded alcohols and a clearing agent, infiltrated and embedded in paraffin, sectioned, and stained with toluidine blue. The tissues were examined microscopically. Collagen arthritic ankles were given scores of 0–5 for inflammation, pannus formation, cartilage damage, and bone resorption, where a score of 0 represents normal with increasing numbers representing increasing severity of disease. A detailed description of the scores is given in Supplemental Table 2.

Pharmacokinetic-Pharmacodynamic Analysis

Pharmacokinetic Analysis. The pharmacokinetic parameters for each test agent in rats from the pharmacokinetic satellite groups were estimated using SAAM II (Saam Institute, University of Washington, Seattle, WA). The estimated parameters were used to simulate systemic concentrations of test agents for the various doses/regimens in the AIA and CIA studies described subsequently during the PK-PD modeling process of ankle swelling.

PK-PD Analysis of Ankle Swelling. The PK-PD analysis of ankle swelling was a naive averaged analysis. Briefly, longitudinal ankle diameter data for each dose level from the AIA and CIA efficacy studies were averaged. The longitudinal average ankle diameter values were fitted to an indirect response model (Fig. 1A), as described by the following differential equation (eq. 1):

$$\frac{d(\mathrm{AD})}{dt} = k_{\mathrm{in}} - I_{\mathrm{AS}}(\mathrm{AD} - \mathrm{AD}_{\mathrm{initial}}) \quad (1)$$

where AD is the ankle diameter (inches); $AD_{initial}$ is the initial ankle diameter on day 0 (inches); t is time (day); k_{in} is the rate of increase in ankle diameter (inches $\times$ day^{-1}); and I_{AS} is the rate constant describing the reduction of ankle swelling by the drugs used in the AIA and CIA studies (day^{-1}).

For studies where the anti-ankle swelling effect of the agent of interest was saturable, I_{AS} was defined by eq. 2:

$$I_{\mathrm{AS}} = \frac{I_{\max} \times C}{\mathrm{IC}_{50} + C} \quad (2)$$

where I_{max} is the maximum value of I_{AS} (day^{-1}); C is the concentration of the test agent; and IC_{50} is the concentration of the test agent where I_{AS} is 50% of I_{max}. For studies where the anti-ankle swelling effect was linear, I_{AS} was defined by eq. 3:

$$I_{\mathrm{AS}} = I \times C \quad (3)$$

where I is a constant that relates the test agent concentration to I_{AS} (μM^{-1} $\times$ day^{-1}).

The choice of using a saturable effect (eq. 2) versus a linear effect (eq. 3) was based on reduction of fitting statistics such as the objective function, Akaike information criterion, and Schwarz-Bayesian information criterion. Both models assume that drug action works to decrease the rate of increase in ankle swelling, which is consistent with what is known about the drugs that are modeled. Pharmacodynamic parameters are presented as the estimate followed by the coefficient of variation in parentheses (Supplemental Table 3). Species differences in plasma protein binding were not considered in the PK-PD analysis since plasma protein binding of the drugs evaluated were comparable based on published literature.

Simulations of clinical regimens/exposures were performed using the PK-PD model and pharmacodynamic parameter estimates from the AIA and CIA studies in combination with human pharmacokinetic parameters obtained from the literature (see Supplemental Table 4), as described in Fig. 1B. Since we were quantitatively evaluating the clinical translatability of AIA and CIA efficacy to clinical activity in patients, the PD parameters estimated from the AIA and CIA studies were used in the clinical simulations. In the simulations, clinically relevant doses and pharmacokinetics were used to simulate the effect of each test agent on the value of AUC_{ankle}. The AUC_{ankle} values for the mean ankle diameter versus time data from vehicle and treatment groups were determined using the trapezoid rule (Gibaldi and Perrier, 1982) and were assessed from study days 1–8. The percentage of inhibition of AUC_{ankle} was determined using eq. 4:

$$\%\mathrm{inhibition\_AUC}_{\mathrm{ankle}} = \frac{\mathrm{AUC}_{\mathrm{vehicle}} - \mathrm{AUC}_{\mathrm{treatment}}}{\mathrm{AUC}_{\mathrm{vehicle}} - \mathrm{AUC}_{\mathrm{normal}}} \times 100\% \quad (4)$$

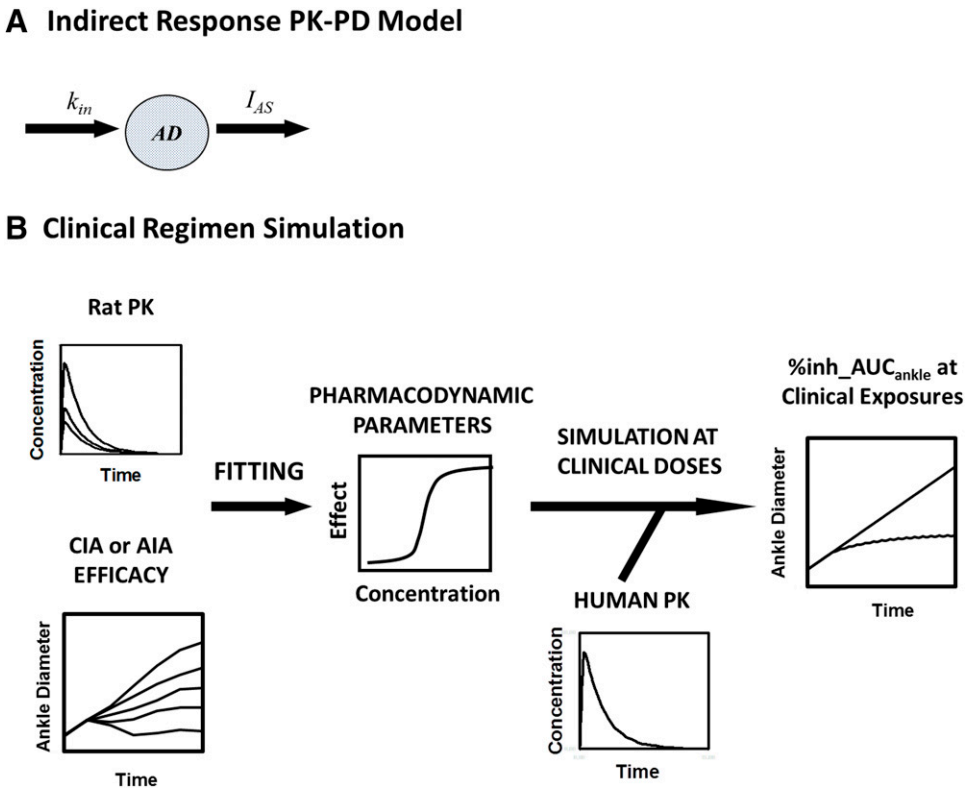

Fig. 1. The PK-PD modeling and simulation process used to translate preclinical ankle joint swelling measurements is depicted. Ankle joint swelling in AIA or CIA rats was described using a standard indirect response model (A). AD (inches) is defined as the ankle diamater, k_{in} (inches $\times$ day^{-1}) is the rate of increase in ankle diameter, and I_{AS} (day^{-1}) is the rate constant describing the anti-ankle joint swelling effect of the agents used in the AIA and CIA studies. The simulation process integrating human pharmacokinetics is described in (B). Pharmacodynamic parameters relating drug concentration to the anti-ankle joint swelling effect are estimated for each drug tested in AIA and CIA rats following fitting of the indirect response model to ankle diameter measurements using rat pharmacokinetics. Simulations of clinical regimen were carried out using the preclinical PK-PD model, estimated pharmacodynamics parameters from preclinical AIA or CIA studies, and human pharmacokinetics from the literature (see Supplemental Table 1).

where %inhibition_AUC$_{ankle}$ is the percentage of inhibition of AUC$_{ankle}$; AUC$_{vehicle}$ is the AUC$_{ankle}$ value for the vehicle control arthritic group; AUC$_{treatment}$ is the AUC$_{ankle}$ value for the treatment group; and AUC$_{normal}$ is the AUC$_{ankle}$ value for the normal control group (i.e., rats without arthritis receiving vehicle).

PK-PD Analysis of Ankle Histopathology. Individual (i.e., inflammation, pannus, cartilage damage, and bone resorption) or summed ankle histopathology scores for each treatment group were normalized to vehicle control scores and converted to a percentage of inhibition using eq. 5:

$$\%\text{inh\_score} = \left(100 - \frac{\text{score}}{\text{score}_{\text{vehicle}}}\right) \times 100\% \quad (5)$$

where %inh_score is the percentage of inhibition of the ankle histopathology score; score is the histopathology score as described previously for ankle histopathology in the AIA and CIA rats; and score$_{vehicle}$ is the ankle histopathology score for vehicle control rats.

The relationship between the steady-state concentrations of each agent tested and individual or summed ankle histopathology scores in rat CIA or AIA were defined by fitting the ankle histopathology score versus concentration data to either a standard E_{max} equation (eq. 6) or an E_{max} equation with a linear effect component (eq. 7):

$$\%\text{inh\_score} = \frac{E_{\max} \times C_{ss}}{EC_{50} + C_{ss}} \quad (6)$$

$$\%\text{inh\_score} = \frac{E_{\max} \times C_{ss}}{EC_{50} + C_{ss}} \times EC_{ss} \quad (7)$$

where E_{max} is the maximum %inh_score; EC$_{50}$ is the concentration at which the %inh_score is at one-half the maximum value; E is a constant describing a linear component of the relationship between concentration and %inh_score; and C_{ss} is the steady-state concentration. Steady-state concentrations for each dose level in the rat AIA and CIA studies were determined by dividing the steady-state area under the curve of the drug concentration-time profile by the dosing interval. In cases where supporting pharmacokinetic data were not collected for a specific treatment group, linear interpolation was performed to estimate the C_{ss} value. This was performed with reasonable confidence since supporting pharmacokinetic data were gathered for treatment groups that were chosen to specifically cover the entire range of doses (see Table 1). The choice of using an E_{max} equation with (eq. 7) or without (eq. 6) a linear effect component was determined by selection of the particular equation that best minimized the sum of squares of residuals and the S.E. of parameter estimates. Fitting of data from AIA or CIA studies was performed using GraphPad Prism version 4.02 (GraphPad Software Inc., San Diego, CA). The estimated pharmacodynamic parameters for ankle histopathology summed scores (AHSS) are presented in Supplemental Table 5.

Following fitting of the ankle histopathology score versus concentration data from the AIA and CIA studies, the percentage of inhibition of ankle histopathology scores at clinically active concentrations of the various test agents was determined. In brief, the estimated parameters from fitting of the ankle histopathology-concentration data were fixed, clinically relevant steady-state concentrations for each test agent were obtained from the literature (see Table 2), and either eq. 6 or 7 was used to interpolate the %inh_score at the clinically relevant steady-state concentrations. Analysis of individual histopathology scores in rat CIA or AIA provided nearly identical conclusions to analysis of summed ankle histopathology scores. Therefore, only the analysis of AHSS is presented in this paper.

Results

Characterization of Dose-Efficacy Relationship in Preclinical Rat Arthritis Models

A range of doses of indomethacin, methotrexate, etanercept, tofacitinib, and dexamethasone was administered to AIA and CIA rats with established disease. Normal control rats treated with vehicle were included in all studies but showed no appreciable change in ankle diameter over the course of the

TABLE 2

Therapeutic dose, percentage of inhibition of AUC_{ankle} following simulations using clinical regimens, steady-state concentration, and corresponding percentage of inhibition of ankle histopathology summed scores

Drug	Therapeutic Dose	% Inhibition of AUC_{ankle}		C_{ss} averge	% Inhibition AHSS	
		AIA	CIA		AIA	CIA
		%	%		%	%
Indomethacin	25 mg three times daily	40	52	1.12 μM[a]	41	45
Methotrexate	7.5 mg once weekly	8	7	0.0133 μM[b]	~8	~5
Etanercept	50 mg once weekly	5	16	1.77 μg/ml[c]	14	29
Tofacitinib	5 mg twice daily	27	63	0.0580 μM[d]	22	56

[a]From Helleberg (1981).
[b]Calculated using AUC/τ and data from Godfrey et al. (1998).
[c]Calculated using AUC/τ and data from Keystone et al. (2004).
[d]Determined by simulating a 5-mg twice daily dose using data from Cohen et al. (2010).
AUC/T = area under the concentration time profile/ dosing interval.

study (Figs. 2–6). The detailed results of these studies are described in the following sections for each drug.

Indomethacin.

AIA. Figure 2A is a representative ankle diameter versus time plot for diseased animals treated with indomethacin (vehicle, and 0.1, 0.3, 1, 3, and 6 mg/kg, by mouth) on days 1–7 of established disease. Daily ankle diameter measurements were significantly ($P < 0.05$) reduced toward normal for AIA rats given indomethacin doses of 0.1 mg/kg (days 5–8), 0.3 mg/kg (days 3–8), 1 mg/kg (days 3–8), and 3 mg/kg (days 2–8) when compared with vehicle control rats. AIA rats treated with 6 mg/kg indomethacin had significantly ($P < 0.05$) reduced ankle diameter measurements (on days 2–5) prior to being euthanized on day 5 due to intolerability. The AUC_{ankle} value was significantly ($P < 0.05$) and dose responsively reduced toward normal for AIA rats treated with indomethacin at doses of 0.1 mg/kg (22% reduction), 0.3 mg/kg (46% reduction), 1 mg/kg (59% reduction), and 3 mg/kg (66% reduction) when compared with vehicle controls. The AUC_{ankle} value was not determined for the 6 mg/kg dose since the dose was tolerated only until day 5. Indomethacin treatment resulted in a dose-dependent decrease in ankle histopathology scores in AIA rats (see Fig. 2B). All individual ankle histopathology parameters (inflammation, pannus, cartilage damage, and bone resorption) were significantly ($P < 0.05$) reduced relative to the vehicle control for AIA rats treated with 3 and 6 mg/kg indomethacin. AIA rats treated with 1 mg/kg indomethacin had significantly ($P < 0.05$) reduced ankle inflammation (44% reduction), cartilage damage (41% reduction), and bone resorption (54% reduction). At 0.3 mg/kg, only the decrease in ankle inflammation (30%) was significant. Accordingly, the effect of indomethacin on summed ankle histopathology scores relative to the vehicle control AIA rats was dose dependent across the entire range of doses tested, and

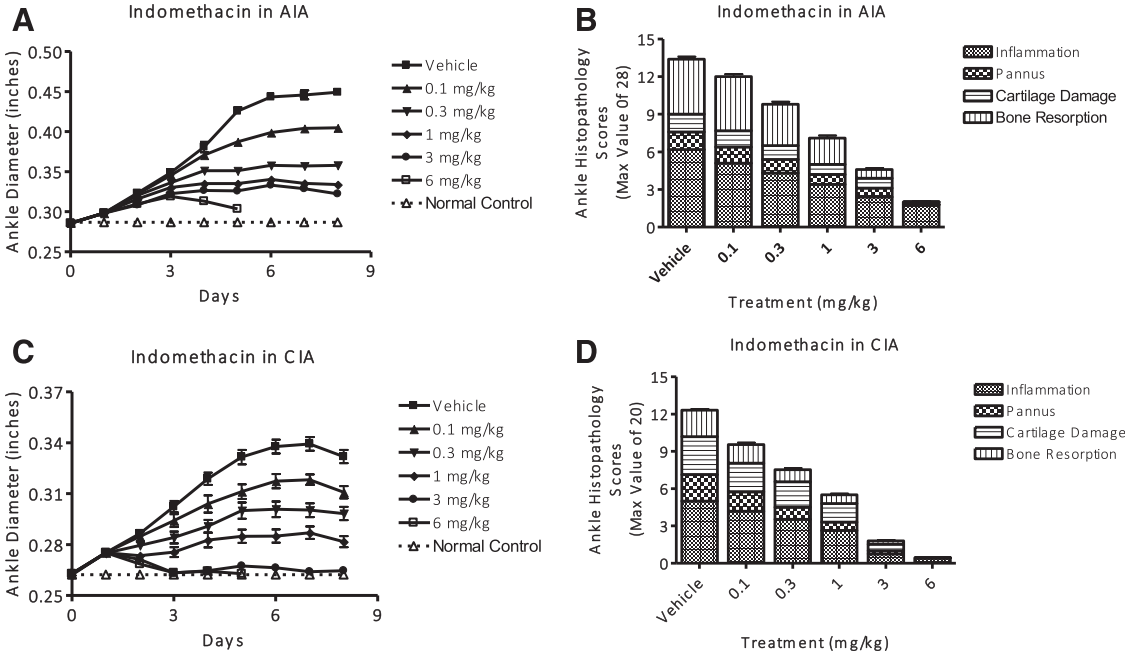

Fig. 2. Ankle diameter vs. time profile in AIA (A) and CIA (C) rats given 0.1, 0.3, 1, 3, or 6 mg/kg indomethacin, by mouth daily, on days 1–7 of established disease. Corresponding end of study ankle histopathology scores in AIA (B) and CIA (D) rats following indomethacin treatment. Each histology parameter (inflammation, pannus, cartilage damage, and bone resorption) is scored from 0 to 7 for AIA rats and 0 to 5 for CIA rats, and is represented by the patterned bars indicated in the legend. Total height of each bar represents the mean summed ankle histopathology score for the specific dose group that can have a maximum value of 28 for AIA rats and 20 for CIA rats. Error bars in the plots represent S.E.M.

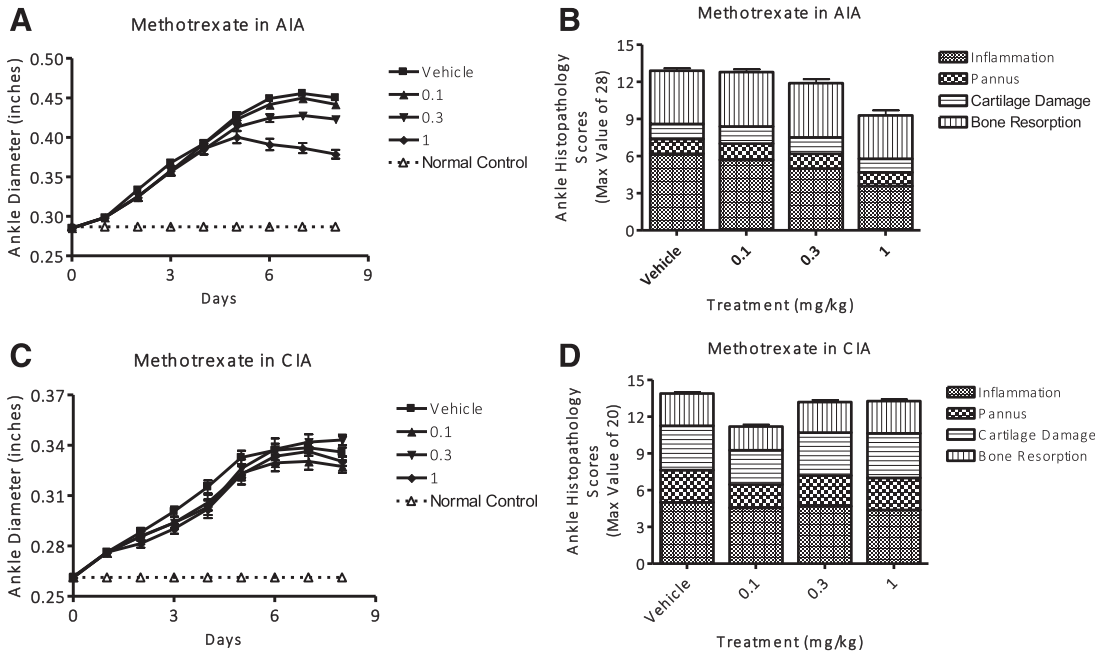

Fig. 3. Ankle diameter vs. time profile in AIA (A) and CIA (C) rats given 0.1, 0.3, 1, 3, or 10 mg/kg methotrexate, by mouth daily, on days 1–7 of established disease. Corresponding end of study ankle histopathology scores in AIA (B) and CIA (D) rats following methotrexate treatment. Each histology parameter (inflammation, pannus, cartilage damage, and bone resorption) is scored from 0 to 7 for AIA rats and 0 to 5 for CIA rats, and is represented by the patterned bars indicated in the legend. Total height of each bar represents the mean summed ankle histopathology score for the specific dose group that can have a maximum value of 28 for AIA rats and 20 for CIA rats. Error bars in the plots represent S.E.M.

was significant ($P < 0.05$) for doses of indomethacin at 1 mg/kg (47% reduction), 3 mg/kg (66% reduction), and 6 mg/kg (86% reduction).

CIA. Figure 2C is a representative ankle diameter versus time plot for diseased animals treated with indomethacin (vehicle, and 0.1, 0.3, 1, 3, and 6 mg/kg, by mouth) on days 1–7 of established disease. Daily ankle diameter measurements were significantly ($P < 0.05$) reduced toward normal for CIA rats given indomethacin doses of 0.1 mg/kg (days 4–8), 0.3 mg/kg (days 2–8), 1 mg/kg (days 2–8), and 3 mg/kg (days 2–8) when compared with vehicle control rats. CIA rats treated with 6 mg/kg indomethacin had significantly ($P < 0.05$) reduced ankle diameter measurements (on days 2–5) prior to being euthanized on day 5 due to intolerability. The AUC_{ankle} value was significantly ($P < 0.05$) and dose responsively reduced toward normal for CIA rats treated with indomethacin at doses of 0.1 mg/kg (25% reduction), 0.3 mg/kg (46% reduction), 1 mg/kg (66% reduction), and 3 mg/kg (92% reduction) when compared with vehicle controls. The AUC_{ankle} value was not determined for the 6 mg/kg dose since the dose was tolerated only until day 5. Indomethacin treatment resulted in a dose-dependent decrease in ankle histopathology scores in CIA rats (see Fig. 2D). All individual ankle histopathology parameters (inflammation, pannus, cartilage damage, and bone resorption) were significantly ($P < 0.05$) reduced relative to the vehicle controls for CIA rats treated with 1, 3, and 6 mg/kg indomethacin. CIA rats treated with 0.3 mg/kg indomethacin had significantly ($P < 0.05$) reduced ankle pannus (54% reduction) and bone resorption (54% reduction). Accordingly, the effect of indomethacin on summed ankle histopathology scores relative to the vehicle control AIA rats was dose dependent and significant ($P < 0.05$) for doses of indomethacin at 0.3 mg/kg (39% reduction), 1 mg/kg (55% reduction), 3 mg/kg (85% reduction), and 6 mg/kg (96% reduction). The effects of indomethacin were slightly more pronounced at similar doses in CIA rats when compared with AIA rats (Fig. 2).

Methotrexate.

AIA. Figure 3A is a representative ankle diameter versus time plot for diseased animals treated with methotrexate (vehicle, and 0.1, 0.3, and 1 mg/kg, by mouth) on days 1–7 of established disease. Daily ankle diameter measurements were significantly ($P < 0.05$) reduced toward normal for AIA rats given methotrexate at 0.3 mg/kg (days 6–8) and 1 mg/kg (days 5–8). The AUC_{ankle} value was significantly ($P < 0.05$) and dose responsively reduced toward normal for AIA rats treated with methotrexate at doses of 0.3 mg/kg (14% reduction) and 1 mg/kg (27% reduction) when compared with vehicle controls. Treatment with 1 mg/kg methotrexate to AIA rats resulted in significantly ($P < 0.05$) reduced ankle inflammation (41% reduction) (see Fig. 3B). The effect of methotrexate on summed ankle histopathology scores relative to the vehicle control AIA rats was significant ($P < 0.05$) only at a dose of 1 mg/kg methotrexate (28% reduction).

CIA. Figure 3C is a representative ankle diameter versus time plot for diseased animals treated with methotrexate (vehicle, and 0.1, 0.3, and 1 mg/kg, by mouth) on days 1–7 of established disease. No significant changes in daily ankle diameter measurements or AUC_{ankle} values were observed. The effect of methotrexate on ankle histopathology scores in CIA rats is shown in Fig. 3D. No significant effects of methotrexate on ankle histopathology were observed. Overall, methotrexate had less of an effect on CIA rats when compared with AIA rats.

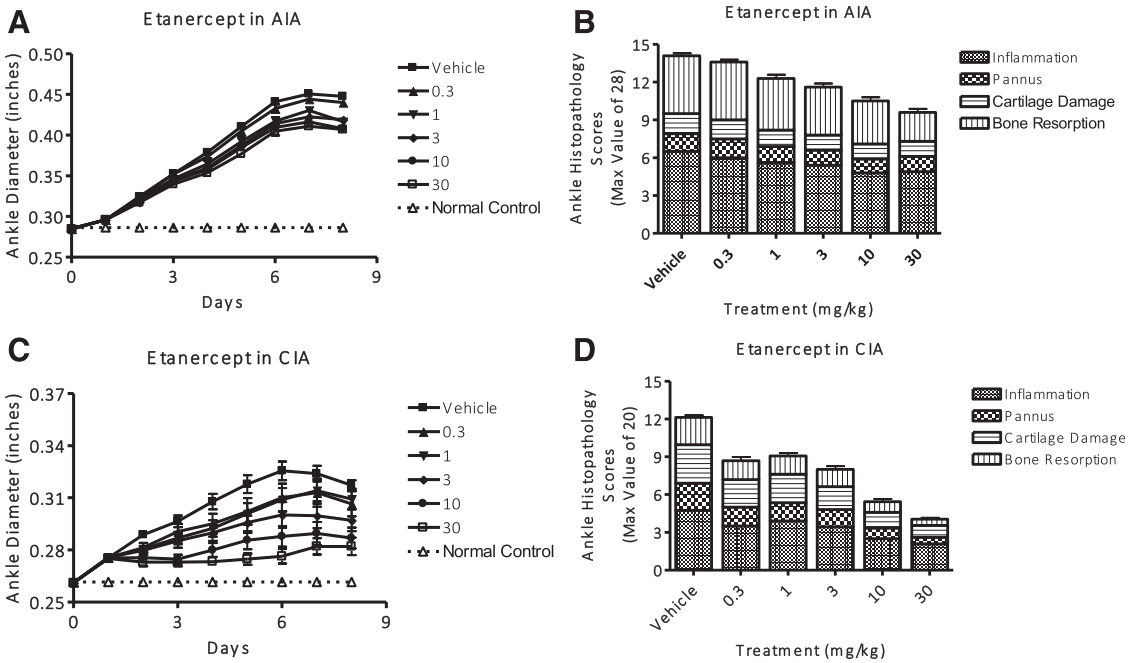

Fig. 4. Ankle diameter vs. time profile in AIA (A) and CIA (C) rats given 0.3, 1, 3, 10, or 30 mg/kg etanercept via subcutaneous injection every third day on days 1, 4, and 7 of established disease. Corresponding end of study ankle histopathology scores in AIA (B) and CIA (D) rats following etanercept treatment. Each histology parameter (inflammation, pannus, cartilage damage, and bone resorption) is scored from 0 to 7 for AIA rats and 0 to 5 for CIA rats, and is represented by the patterned bars indicated in the legend. Total height of each bar represents the mean summed ankle histopathology score for the specific dose group that can have a maximum value of 28 for AIA rats and 20 for CIA rats. Error bars in the plots represent S.E.M.

Etanercept.

AIA. Figure 4A is a representative ankle diameter versus time plot for diseased animals treated with etanercept (vehicle, and 0.3, 1, 3, 10, and 30 mg/kg) by subcutaneous injection on days 1, 4, and 7 of established disease. Daily ankle diameter measurements were significantly ($P < 0.05$) reduced toward normal for AIA rats given etanercept doses of 1 mg/kg (days 6–8), 3 mg/kg (days 4–8), 10 mg/kg (days 4–8), and 30 mg/kg (days 4–8) when compared with vehicle control rats. The AUC_{ankle} value was significantly ($P < 0.05$) and dose responsively reduced toward normal for AIA rats treated with etanercept at doses of 1 mg/kg (14% reduction), 3 mg/kg (17% reduction), 10 mg/kg (20% reduction), and 30 mg/kg (24% reduction) when compared with vehicle controls. Etanercept treatment resulted in a dose-dependent decrease in ankle histopathology scores in AIA rats (see Fig. 4B). AIA rats treated with 10 mg/kg etanercept had significantly ($P < 0.05$) reduced ankle inflammation (26% reduction). At 30 mg/kg, etanercept significantly reduced both ankle inflammation (25% reduction) and bone resorption (49% reduction). The effect of etanercept on summed ankle histopathology scores relative to the vehicle control AIA rats was dose dependent and significant ($P < 0.05$) at etanercept doses of 10 mg/kg (25% reduction) and 30 mg/kg (32% reduction).

CIA. Figure 4C is a representative ankle diameter versus time plot for diseased animals treated with etanercept (vehicle, and 0.3, 1, 3, 10, and 30 mg/kg) by subcutaneous injection on days 1, 4, and 7 of established disease. Daily ankle diameter measurements were significantly ($P < 0.05$) reduced toward normal for CIA rats given etanercept doses of 3 mg/kg (days 3–8), 10 mg/kg (days 2–8), and 30 mg/kg (days 2–8) when compared with vehicle control rats. The AUC_{ankle} value was significantly ($P < 0.05$) and dose responsively reduced toward normal for CIA rats treated with etanercept at doses of 3 mg/kg (37% reduction), 10 mg/kg (56% reduction), and 30 mg/kg (69% reduction) when compared with vehicle controls. Etanercept treatment resulted in a dose-dependent decrease in ankle histopathology scores in CIA rats (see Fig. 4D). All individual ankle histopathology parameters (inflammation, pannus, cartilage damage, and bone resorption) were significantly ($P < 0.05$) reduced relative to the vehicle controls for CIA rats treated with 30 mg/kg etanercept. CIA rats treated with 10 mg/kg etanercept had significantly ($P < 0.05$) reduced ankle pannus (61% reduction), cartilage damage (59% reduction), and bone resorption (61% reduction). Accordingly, the effect of etanercept on summed ankle histopathology scores relative to the vehicle control AIA rats was dose dependent but significant ($P < 0.05$) only at an etanercept dose of 30 mg/kg (66% reduction). The effects of etanercept were more pronounced in CIA rats when compared with AIA rats (Fig. 4).

Tofacitinib.

AIA. Figure 5A is a representative ankle diameter versus time plot for diseased animals treated with tofacitinib (vehicle, and 0.5, 1.5, 5, 15, and 45 mg/kg, by mouth) on days 1–7 of established disease. Daily ankle diameter measurements were significantly ($P < 0.05$) reduced toward normal for AIA rats given tofacitinib doses of 0.5 mg/kg (days 6–8), 1.5 mg/kg (days 3–8), 5 mg/kg (days 2–8), 15 mg/kg (days 2–8), and 45 mg/kg (days 2–8) when compared with vehicle control rats. The AUC_{ankle} value was significantly ($P < 0.05$) and dose responsively reduced toward normal for AIA rats treated with tofacitinib at doses of 1.5 mg/kg (19% reduction), 5 mg/kg (34% reduction), 15 mg/kg (47% reduction), and 45 mg/kg (66% reduction) when compared with vehicle controls. Tofacitinib treatment resulted in a dose-dependent decrease in ankle histopathology scores in AIA rats (see Fig. 5B). All individual

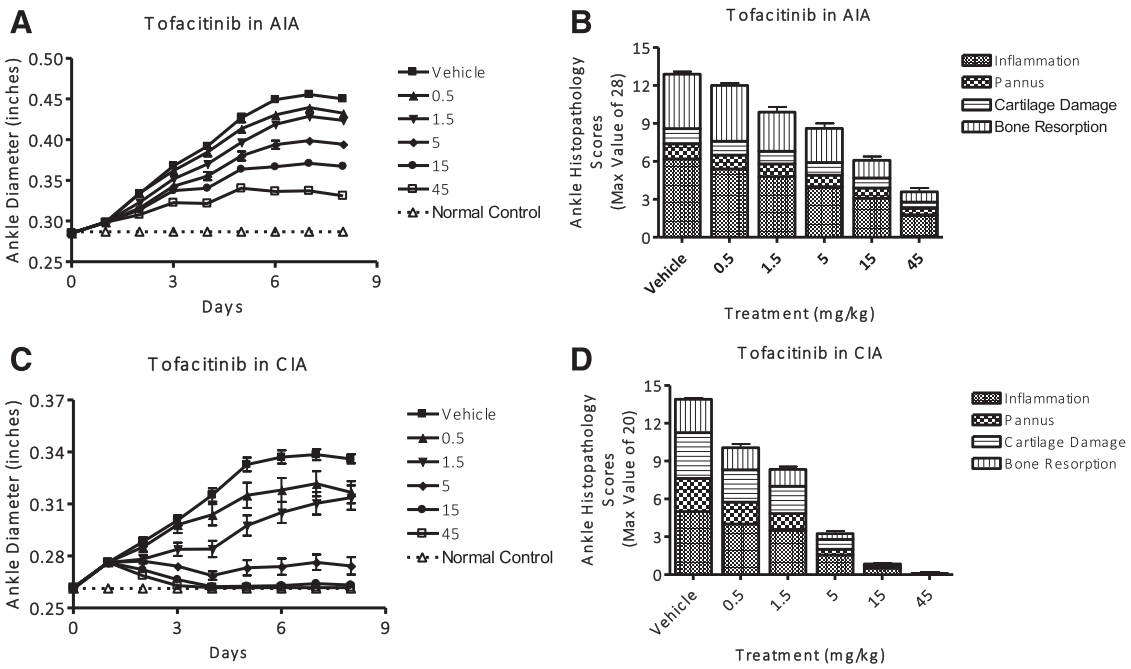

Fig. 5. Ankle diameter vs. time profile in AIA (A) and CIA (C) rats given 0.5, 1.5, 5, 15, or 45 mg/kg tofacitinib, by mouth daily, on days 1–7 of established disease. Corresponding end of study ankle histopathology scores in AIA (B) and CIA (D) rats following tofacitinib treatment. Each histology parameter (inflammation, pannus, cartilage damage, and bone resorption) is scored from 0 to 7 for AIA rats and 0 to 5 for CIA rats, and is represented by the patterned bars indicated in the legend. Total height of each bar represents the mean summed ankle histopathology score for the specific dose group that can have a maximum value of 28 for AIA rats and 20 for CIA rats. Error bars in thr plots represent S.E.M.

ankle histopathology parameters (inflammation, pannus, cartilage damage, and bone resorption) were significantly ($P < 0.05$) reduced relative to the vehicle control for AIA rats treated with 45 mg/kg tofacitinib. AIA rats treated with 15 mg/kg tofacitinib had significantly ($P < 0.05$) reduced ankle inflammation (51% reduction) and bone resorption (67%). At 5 mg/kg, only the decrease in ankle inflammation (35%) was significant. The effect of tofacitinib on summed ankle histopathology scores relative to the vehicle control AIA rats was dose dependent across the entire range of doses tested and significant ($P < 0.05$) at tofacitinib doses of 5 mg/kg (33% reduction), 15 mg/kg (52% reduction), and 45 mg/kg (72% reduction).

CIA. Figure 5C is a representative ankle diameter versus time plot for diseased animals treated with tofacitinib (vehicle, and 0.5, 1.5, 5, 15, and 45 mg/kg, by mouth) on days 1–7 of established disease. Daily ankle diameter measurements were significantly ($P < 0.05$) reduced toward normal for CIA rats given tofacitinib doses of 0.5 mg/kg (days 6–8), 1.5 mg/kg (days 2–8), 5 mg/kg (days 2–8), 15 mg/kg (days 2–8), and 45 mg/kg (days 2–8) when compared with vehicle control rats. The AUC_{ankle} value was significantly ($P < 0.05$) and dose responsively reduced toward normal for CIA rats treated with tofacitinib at doses of 1.5 mg/kg (42% reduction), 5 mg/kg (77% reduction), 15 mg/kg (92% reduction), and 45 mg/kg (95% reduction) when compared with vehicle controls. Tofacitinib treatment resulted in a dose-dependent decrease in ankle histopathology scores in CIA rats (see Fig. 5D). All individual ankle histopathology parameters (inflammation, pannus, cartilage damage, and bone resorption) were significantly ($P < 0.05$) reduced relative to the vehicle controls for CIA rats treated with 5, 15, and 45 mg/kg tofacitinib. CIA rats treated with 1.5 mg/kg tofacitinib had significantly ($P < 0.05$) reduced ankle pannus (49% reduction) and bone resorption (49% reduction). Accordingly, the effect of tofacitinib on summed ankle histopathology scores relative to the vehicle control CIA rats was dose dependent and significant ($P < 0.05$) at tofacitinib doses of 1.5 mg/kg (40% reduction), 5 mg/kg (77% reduction), 15 mg/kg (94% reduction), and 45 mg/kg (100% reduction). The effects of tofacitinib were more pronounced at similar doses in CIA rats when compared with AIA rats (Fig. 5).

Dexamethasone.

AIA. Figure 6A is a representative ankle diameter versus time plot for diseased animals treated with dexamethasone (vehicle, and 0.0125, 0.025, 0.05, 0.1, and 0.2 mg/kg, by mouth) on days 1–7 of established disease. Daily ankle diameter measurements were significantly ($P < 0.05$) reduced toward normal for AIA rats given dexamethasone doses of 0.0125 mg/kg (day 4), 0.025 mg/kg (days 3–8), 0.05 mg/kg (days 2–8), 0.1 mg/kg (days 2–8), and 0.2 mg/kg (days 2–8) when compared with vehicle control rats. The AUC_{ankle} value was significantly ($P < 0.05$) and dose responsively reduced toward normal for AIA rats treated with dexamethasone at doses of 0.025 mg/kg (27% reduction), 0.05 mg/kg (39% reduction), 0.1 mg/kg (58% reduction), and 0.2 mg/kg (82% reduction) when compared with vehicle controls. Dexamethasone treatment resulted in a dose-dependent decrease in ankle histopathology scores in AIA rats (see Fig. 6B). All individual ankle histopathology parameters (inflammation, pannus, cartilage damage, and bone resorption) were significantly ($P < 0.05$) reduced relative to the vehicle control for AIA rats treated with 0.05, 0.1, and 0.2 mg/kg dexamethasone. AIA rats treated with 0.025 mg/kg dexamethasone had significantly ($P < 0.05$) reduced ankle inflammation (23% reduction) and bone resorption (42% reduction). The

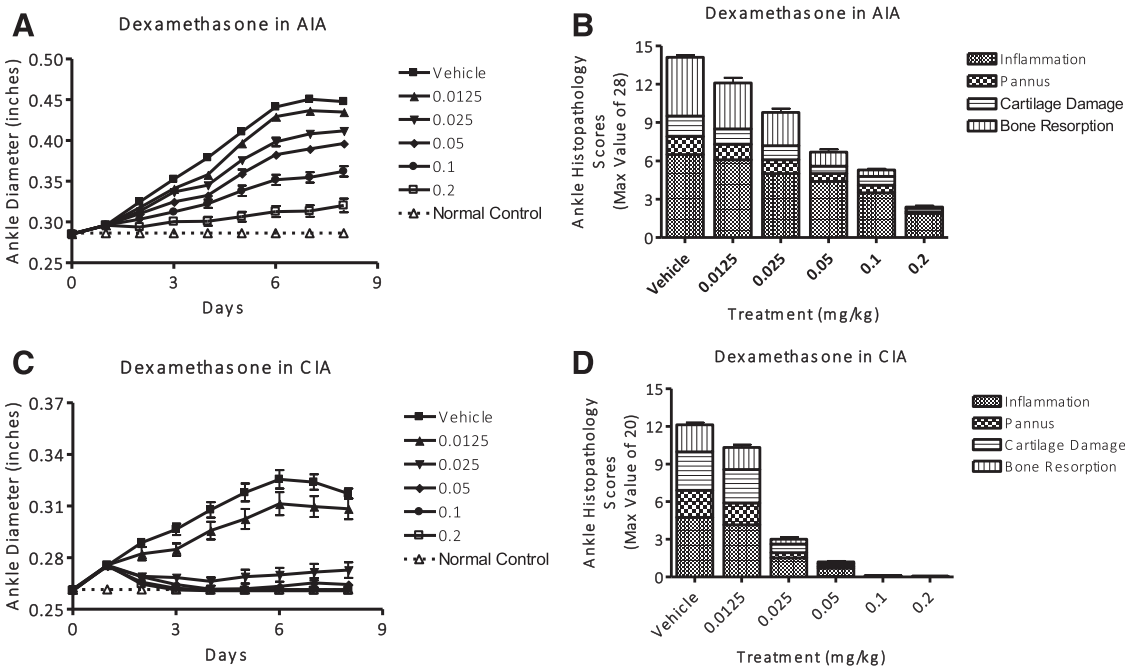

Fig. 6. Ankle diameter vs. time profile in AIA (A) and CIA (C) rats given 0.0125, 0.025, 0.05, 0.1, or 0.2 mg/kg dexamethasone, by mouth daily, on days 1–7 of established disease. Corresponding end of study ankle histopathology scores in AIA (B) and CIA (D) rats following dexamethasone treatment. Each histology parameter (inflammation, pannus, cartilage damage, and bone resorption) is scored from 0 to 7 for AIA rats and 0 to 5 for CIA rats, and is represented by the patterned bars indicated in the legend. Total height of each bar represents the mean summed ankle histopathology score for the specific dose group that can have a maximum value of 28 for AIA rats and 20 for CIA rats. Error bars in the plots represent S.E.M.

effect of dexamethasone on summed ankle histopathology scores relative to the vehicle control AIA rats was dose dependent across the entire range of doses tested and significant ($P < 0.05$) at dexamethasone doses of 0.025 mg/kg (30% reduction), 0.05 mg/kg (52% reduction), 0.1 mg/kg (62% reduction), and 0.2 mg/kg (83% reduction).

CIA. Figure 6C is a representative ankle diameter versus time plot for diseased animals treated with dexamethasone (vehicle, and 0.0125, 0.025, 0.05, 0.1, and 0.2 mg/kg, by mouth) on days 1–7 of established disease. Daily ankle diameter measurements were significantly ($P < 0.05$) reduced toward normal for CIA rats given dexamethasone doses of 0.0125 mg/kg (day 3), 0.025 mg/kg (days 2–8), 0.05 mg/kg (days 2–8), 0.1 mg/kg (days 2–8), and 0.2 mg/kg (days 2–8) when compared with vehicle control rats. The AUC_{ankle} value was significantly ($P < 0.05$) and dose responsively reduced toward normal for CIA rats treated with dexamethasone at doses of 0.025 mg/kg (82% reduction), 0.05 mg/kg (92% reduction), 0.1 mg/kg (96% reduction), and 0.2 mg/kg (98% reduction) when compared with vehicle controls. Dexamethasone treatment resulted in a dose-dependent decrease in ankle histopathology scores in CIA rats (see Fig. 6D). All individual ankle histopathology parameters (inflammation, pannus, cartilage damage, and bone resorption) were significantly ($P < 0.05$) reduced relative to the vehicle controls for CIA rats treated with 0.025, 0.05, 0.1, and 0.2 mg/kg dexamethasone. Accordingly, the effect of dexamethasone on summed ankle histopathology scores relative to the vehicle control CIA rats was dose dependent and significant ($P < 0.05$) at dexamethasone doses of 0.025 mg/kg (75% reduction), 0.05 mg/kg (90% reduction), 0.1 mg/kg (99% reduction), and 0.2 mg/kg (99% reduction). The effects of dexamethasone were more pronounced at similar doses in CIA rats when compared with AIA rats (Fig. 6).

Anti-Inflammatory Activity on Ankle Swelling

Characterization of anti-inflammatory activity on ankle swelling in AIA and CIA rats of systemic concentrations of indomethacin, methotrexate, etanercept, and tofacitinib was determined through a PK-PD modeling approach. Dexamethasone AIA and CIA studies were not included in this analysis since corticosteroids are typically administered as acute local injections making relationships between systemic concentrations and drug effect less clinically relevant. A PK-PD model (Fig. 1A) characterizing systemic drug effect (for details, see *Materials and Methods*) was used to fit ankle diameter data from preclinical studies. The indirect response PK-PD model described by the equation in Fig. 1A assumes that a drug acts to reduce ankle swelling through increasing the rate constant, I_{AS}. The choice of using an antiarthritis effect described by a saturable equation (eq. 2) versus a linear equation (eq. 3) was based on model-fitting statistics (see *Materials and Methods*). Inflammation and subsequent ankle swelling appeared to have a faster onset rate in AIA rats and was reflected in k_{in} estimates that were approximately 2-fold higher in AIA compared with CIA rats in all studies (Supplemental Table 3). There was good concordance between the predicted ankle diameter obtained from the PK-PD fits and observed ankle diameters, indicating that the PK-PD models used adequately characterize drug effects on ankle inflammation in AIA (Fig. 7C) and CIA rats (Fig. 7D).

Direct comparisons of pharmacodynamic parameters reflective of anti-inflammatory activity on ankle swelling could not be made across all antiarthritis agents tested since the PK-PD models used to characterize each agent were often not identical (see Supplemental Table 3). However, comparisons of anti-inflammatory activity relative to clinically relevant

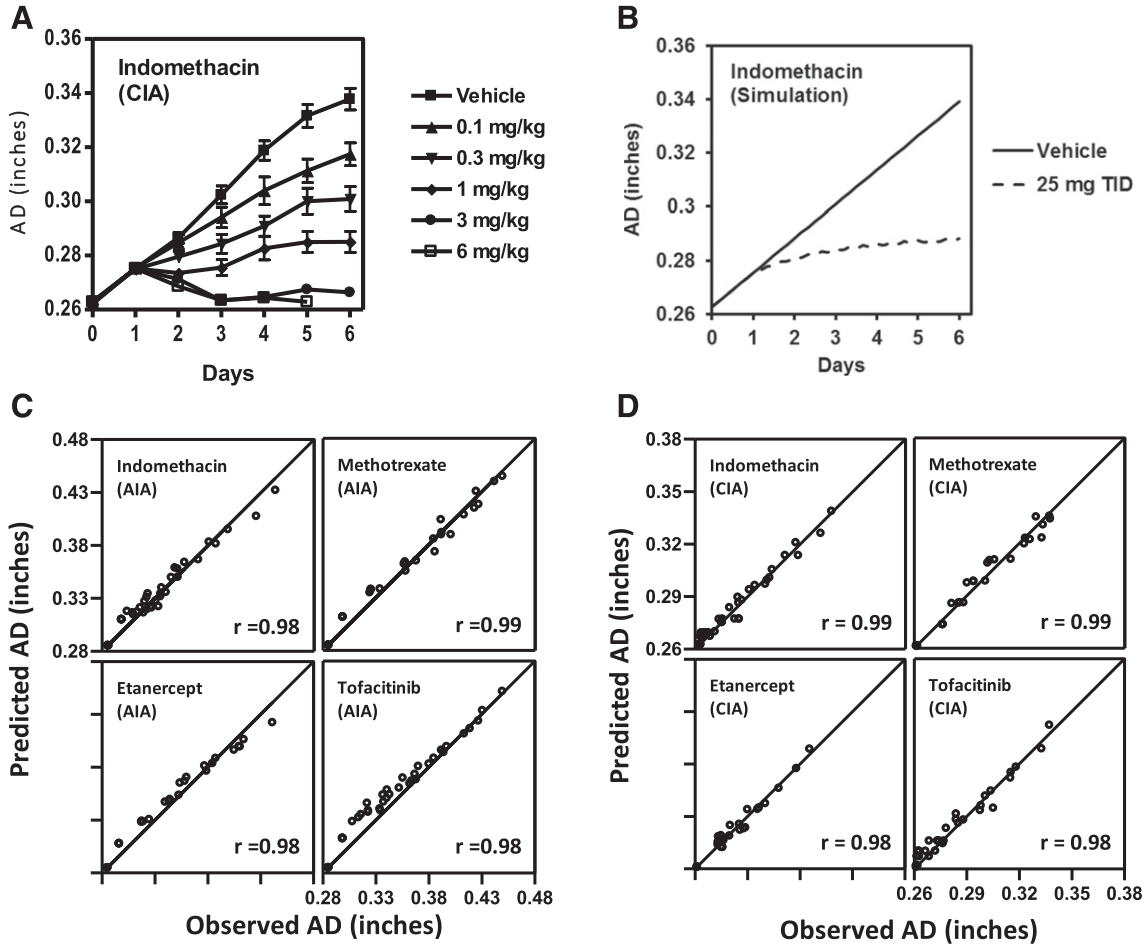

Fig. 7. An example of a PK-PD analysis of ankle swelling from a rat arthritis model study is shown. (A) Representative plot of mean AD vs. time for the dosing ranging study with indomethacin in rat CIA up to study day 6. (B) Representative simulation of clinical regimen of indomethacin using human pharmacokinetics as described in Fig. 1B. (C) Plots of PK-PD model–predicted mean AD vs. observed AD in AIA rats given indomethacin, methotrexate, etanercept, and tofacitinib. (D) Plots of PK-PD model–predicted mean AD vs. observed AD in CIA rats given indomethacin, methotrexate, etanercept, and tofacitinib. Error bars in the plots represent S.E.M.

exposures could be accomplished through simulations using the preclinical PK-PD models and clinical pharmacokinetics, dose, and regimen (see Fig. 1B). Figure 7, A and B shows a representative CIA ankle diameter-time profile and an associated PK-PD model ankle diameter simulation using a clinical regimen for indomethacin. Table 2 summarizes the percentage of inhibition of the ankle diameter area under the curve (i.e., AUC_{ankle}) following clinical regimen simulations for indomethacin, methotrexate, etanercept, and tofacitinib. None of the agents tested inhibited AUC_{ankle} completely. Indomethacin and tofacitinib appear to be the most active agents in both preclinical models, with maximum inhibition of AUC_{ankle} being 52% and 63% in CIA rats, respectively. Inhibition of AUC_{ankle} by indomethacin and tofacitinib was less in AIA rats (40% and 27%, respectively). The diminished anti-inflammatory activity in AIA rats appears to be a consequence of more aggressive inflammation in AIA rats, as evidenced by the approximately 2-fold higher k_{in} value in AIA compared with CIA rats mentioned previously. Inhibition of AUC_{ankle} by methotrexate and etanercept at clinically relevant exposures was less effective compared with indomethacin and tofacitinib, being ≤16% in both AIA and CIA rats.

Ankle Histopathology at Clinically Relevant Exposures

Characterization of relationships between AHSS and systemic drug concentrations of indomethacin, etanercept, and tofacitinib was performed using either the standard E_{max} equation (eq. 6) or the E_{max} equation with a linear effect component (eq. 7). Dexamethasone AIA and CIA studies were not included in this analysis since corticosteroids are typically administered as acute local injections, making relationships between systemic concentrations and drug effect less clinically relevant. Figure 8 shows plots of the percentage of inhibition of the AHSS versus steady-state drug concentrations and the associated model fitted lines and pharmacodynamics parameters. Of note, the estimated E_{max} value of tofacitinib in CIA (Fig. 8F) exceeded 100% (i.e., 105%), which is not possible by definition. Since this was an estimated value, and very close to the theoretical E_{max} maximum of 100%, we chose to report the value as the fitted estimated value. Methotrexate histopatholgy summed scores were not modeled due to inadequate dose responsiveness characterization for modeling purposes (see Fig. 3, B and D).

Estimated pharmacodynamics parameters were used to calculate the percentage of inhibition of AHSS at clinical

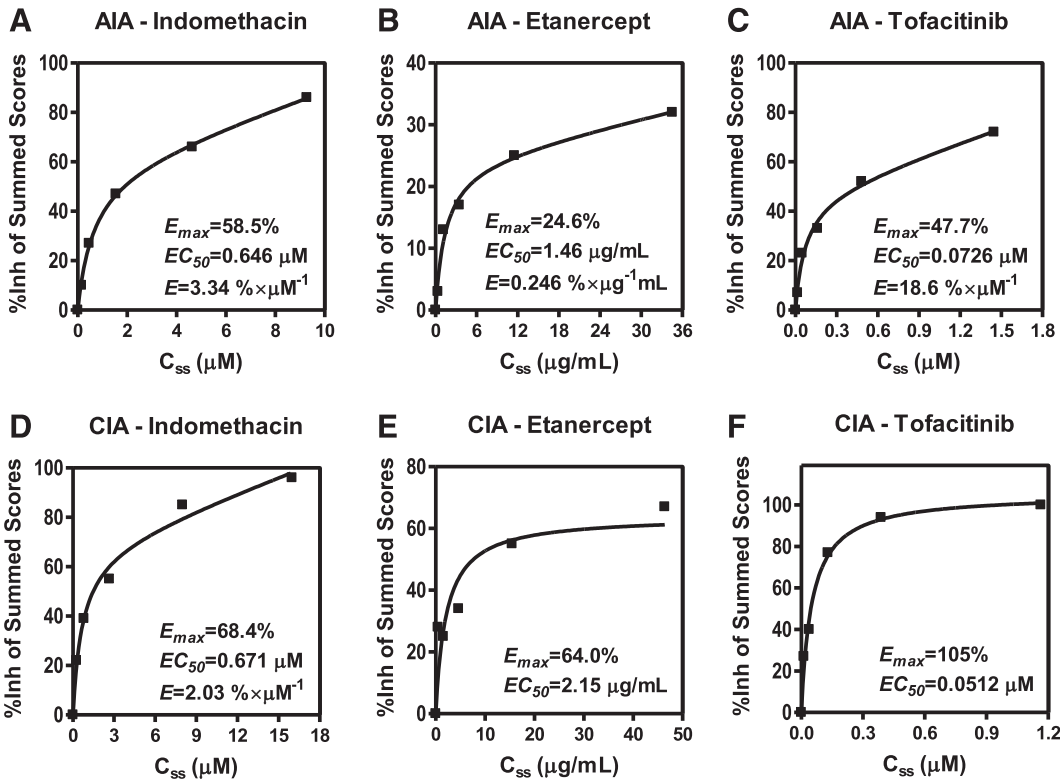

Fig. 8. Plots of AHSS vs. plasma C_{ss} for indomethacin (A and D), etanercept (B and E), and tofacitinib (C and F). Squares represent mean observed data. The solid line represents the model-predicted curve.

steady-state concentrations and the results are presented in Table 2. For methotrexate, the percentage of inhibition of ankle histopathology was approximated by comparing clinical steady-state concentrations to those estimated for each dose level based on the measured pharmacokinetics from the satellite group. The estimated steady-state concentration at the 0.3 mg/kg dose level in both AIA (0.0117 μM) and CIA (0.00832 μM) rats was similar to that estimated in patients (0.0133 μM). Therefore, the percentage of inhibition of AHSS at clinically relevant exposures was approximated to values observed at the 0.3 mg/kg dose in AIA (~8%) and CIA (~5%) rats. Similar to the analysis of anti-inflammatory activity associated with ankle swelling, no antiarthritis agent tested caused complete inhibition of ankle histology at clinically relevant steady-state concentrations. Once again, indomethacin and tofacitinib were the most effective in inhibiting ankle histopathology in CIA rats, resulting in 45% and 56% inhibition of ankle histopathology, respectively. Both drugs caused less inhibition of ankle histopathology in AIA compared with CIA rats, which is likely due to AIA rats exhibiting more aggressive disease. Similar to indomethacin and tofacitinib, etanercept exhibited more activity on ankle histopathology assessments in CIA rats but to a lesser magnitude. Methotrexate was the least active on ankle histopathology of all agents tested.

Discussion

Despite their wide use and acknowledged importance to drug development, the ability of rodent immune-mediated arthritis models to quantitatively predict therapeutic activity of antiarthritis agents is poorly understood. The clinical relevance of rodent immune-mediated arthritis models has been investigated and reviewed by others (Bendele et al., 1999; Kannan et al., 2005; Hegen et al., 2008). However, reported investigations provide qualitative, or at best semi-quantitative, comparisons of preclinical and clinical efficacy since known species differences in pharmacokinetics of anti-arthritis agents were not taken into account. In a recent paper reviewing the use of translational PK-PD analysis in the pharmaceutical industry, a shortage of quantitative clinical validation of translatable-preclinical models was reported for autoimmune diseases including RA (Wong et al., 2017). The current work provides a detailed quantitative examination of drug exposure-effect relations in rat AIA and CIA using PK-PD analysis to evaluate preclinical efficacy within the context of clinically relevant drug exposures. Therapeutic efficacy rather than prophylactic efficacy in AIA and CIA rats was evaluated since therapeutic efficacy has been found to be more predictive of clinical efficacy in human RA patients (Hegen et al., 2008).

The four antirheumatic agents that were used in our evaluation included indomethacin, methotrexate, etanercept (an anti-TNF biologic), and tofacitinib (a recently approved oral Janus kinase inhibitor). Unlike the other drugs evaluated, indomethacin is used to manage symptoms of RA such as pain, stiffness, inflammation, and joint swelling at clinically relevant doses (Saul and Korlipara, 1991; Burke et al., 2006; Combe et al., 2017). Indomethacin is not considered to be a disease-modifying antirheumatic drug; therefore, it is not expected to stop the progression of disease and prevent joint destruction. In contrast, methotrexate (a conventional synthetic DMARD), etanercept (a biologic DMARD), and tofacitinib (a targeted synthetic DMARD) represent different classes of

DMARDS that are used clinically to prevent or reduce the risk of RA-associated joint damage (Chatzidionysiou et al., 2017; Combe et al., 2017; Ramiro et al., 2017). Finally, dexamethasone (a corticosteroid), typically delivered by local injection to RA patients, was included as a common positive control in both preclinical models.

The efficacy endpoints used in our analysis were inhibition of AUC_{ankle} and inhibition of AHSS, since increases in ankle diameter (assessed as increases in AUC_{ankle}) in AIA and CIA rats result from edema of the joint and serve as a measure of inflammation. The AHSS comprised of individual histopathology scores (i.e., inflammation, pannus, cartilage damage, and bone resorption) serves as a measurement of underlying structural changes to the bone caused by disease progression. For each drug tested, inhibition of both AUC_{ankle} and AHSS were generally comparable in both magnitude and rank order (Table 2). Of interest, methotrexate showed the lowest magnitude of effect on AHSS at clinically relevant drug concentrations despite being the standard of care DMARD for the clinical treatment of RA (Combe et al., 2017). Overall, based on both the AUC_{ankle} and AHSS inhibition data, the rank ordering of preclinical activity was tofacitinib $>$ etanercept $\geq$ methotrexate.

Direct comparisons with clinical activity in RA are difficult since assessment of clinical antirheumatic activity is only pseudo-quantitative in nature. However, emerging clinical data are consistent with our rank ordering of drug activity. Tofacitinib monotherapy appears to be more effective than methotrexate in methotrexate naive RA patients (patients who have not previously received methotrexate or therapeutic doses of methotrexate) in the reduction of RA signs and symptoms and inhibiting the progression of structural joint damage (Lee et al., 2014; Strand et al., 2016). Comparisons of the clinical efficacy of etanercept and methotrexate monotherapy were not as clear-cut. A meta-analysis of clinical efficacy data of four anti-TNF biologics including etanercept given as monotherapy compared with methotrexate monotherapy showed that while risk ratios (an efficacy metric) favored the anti-TNF biologics, they do not reach statistical significance (Aaltonen et al., 2012). Similarly, differences between etanercept and methotrexate activity on AHSS were not entirely consistent with both compounds showing similar efficacy in AIA rats, but with etanercept having greater efficacy in CIA rats (Table 2).

As a note of caution, despite the apparent concordance of our preclinical efficacy data for DMARDs to clinical efficacy, the predictive value of preclinical efficacy in AIA and CIA rats is not without flaw. Of note, indomethacin showed equal or often better efficacy than other DMARDs on inhibiting structural joint damage in AIA and CIA rats (as assessed by inhibition of AHSS) despite having limited ability to prevent joint damage clinically in RA patients. The comparable efficacy of indomethacin on both AUC_{ankle} and AHSS serves as a clear example of the inability of AIA and CIA rats to provide differentiation between treatment of disease symptoms (joint inflammation) and disease progression (joint damage) that is observed clinically. Despite this, application of translational PK-PD modeling of preclinical efficacy in AIA and CIA rats does have value in drug development. The translational value of PK-PD analyses can be grouped into two broad categories: 1) rank ordering of new antiarthritis therapies within the context of relevant clinical concentrations and 2) characterization of quantitative relationships of biologic pathways important to RA.

Rank Ordering of New Antiarthritis Therapies within the Context of Relevant Clinical Concentrations. A central theme of our work described in the current paper is the ability of PK-PD analysis to normalize species difference in pharmacokinetics in order to properly context preclinical activity to clinically relevant drug concentrations in humans. In theory, this would allow fair comparison of efficacy of new therapies to existing drugs on the market. The current study suggests that the clinical activity of antirheumatic drugs can be rank ordered based on preclinical activity despite the confounding results with indomethacin. Ideally, rank ordering of compound efficacy is best performed with the following two considerations. First, the appropriate choice of model is important for meaningfully ranking compounds. Since RA is a heterogeneous disease and is likely manifested by different pathologic pathways, RA patients show varying responses to any particular drug therapy that normally interferes with one or few biologic pathways. Thus, the preclinical evaluation of a novel compound's efficacy should be performed in models sharing the appropriate pathologic pathways in human RA. Animal model selection in such a manner would provide a biologically plausible rational for improved efficacy when comparing new drug candidates to either marketed drugs or more advanced compounds targeting the same biologic pathway. Second, testing in more than one model is preferred whenever possible to evaluate the contribution of different genetic backgrounds and inflammatory conditions. An example of a rank ordering approach is described in a case study from a recent paper from the pharmaceutical industry, where preclinical PK-PD analysis of efficacy data in AIA rats was used to rank order and select second-generation drug candidates with anticipated improved efficacy compared with an advanced competitor compound sharing the same mechanism of action (Wong et al., 2017). As a final note, rank ordering of efficacy is likely more reliable when comparing drugs/compounds that share the same biologic target. Furthermore, preclinical models of arthritis differ from human RA in that these models have a more aggressive form of the disease and contributions from various biologic drivers of preclinical disease may differ from human RA. For example, the inflammatory stimuli or pathways that triggered leukocyte influx, joint swelling, and bone damage in these models may differ from those in human RA. Thus, the quantitative assessment of preclinical efficacy endpoints may only be useful for the rank ordering of those relevant pathways in the selected models. For instance, our PK-PD modeling results with methotrexate and etanercept show that at clinically relevant concentrations the preclinical activity in therapeutic AIA and CIA rats is rather low for these two clinically effective DMARDs (Table 2), suggesting the pathogenic contributions of the TNF-α pathway in these models may not be as high as those in human RA.

Characterization of Quantitative Relationships of Biologic Pathways Important to RA. A second aspect of the translational value of PK-PD analysis of preclinical arthritis models involves the quantitative characterization of biologic pathways central to the disease through the development of mechanistic PK-PD models. These mechanistic PK-PD models offer a means to: 1) evaluate the degree of importance of the biologic pathway in an immune-mediated

disease in an in vivo setting; 2) assess the in vitro to in vivo correlation of drug potency; 3) explore new biomarkers that quantitatively assess their modulation with an efficacy outcome; and 4) assess the synergism following inhibition of more than one biologic pathway. Some of these applications have been reported and used in the pharmaceutical industry (Wong et al., 2017). Finally, the resultant mechanistic PK-PD models can be used to influence design of early clinical trials including setting of pharmacodynamic biomarker endpoints, generating therapeutic and toxicity indexes, and providing insights into therapeutic mechanisms related to efficacy.

In summary, the current work describes a comprehensive effort to provide clinical validation of therapeutic AIA and CIA in rats using translational PK-PD analysis. Based on our work, PK-PD analysis of preclinical efficacy data can be used to rank order the clinical efficacy of new therapies for RA. In addition, we propose that PK-PD modeling of preclinical efficacy data improves the quantitative understanding of biologic pathways involved in RA and can provide value in the search for new and novel therapies. Finally, the described approach to clinically validate therapeutic AIA and CIA in rats can be applied to other animal models of autoimmune disease.

Acknowledgments

The authors thank Dr. Alison Bendele of Bolder BioPATH, Inc. (Boulder, CO) for assistance with the conduct of the preclinical studies. We also thank Dr. John C. Davis, Jr., Dr. William Kennedy, and Dr. Donna M. Dambach for insightful discussions, as well as Dr. Laura DeForge, Rashi Takkar, and Jianyong Wang for assistance in the measurement of etanercept concentrations.

Authorship Contributions

Participated in research design: Wong, Hop.

Conducted experiments: Deng.

Contributed new reagents or analytic tools: Deng.

Performed data analysis: Wong, Liu, Ouyang, Wright, Hop.

Wrote or contributed to the writing of the manuscript: Wong, Liu, Ouyang, Deng, Wright, Hop.

References

Aaltonen KJ, Virkki LM, Malmivaara A, Konttinen YT, Nordström DC, and Blom M (2012) Systematic review and meta-analysis of the efficacy and safety of existing TNF blocking agents in treatment of rheumatoid arthritis. *PLoS One* **7**:e30275.

Arrowsmith J and Miller P (2013) Trial watch: phase II and phase III attrition rates 2011–2012. *Nat Rev Drug Discov* **12**:569.

Bendele A (2001) Animal models of rheumatoid arthritis. *J Musculoskelet Neuronal Interact* **1**:377–385.

Bendele A, McComb J, Gould T, McAbee T, Sennello G, Chlipala E, and Guy M (1999) Animal models of arthritis: relevance to human disease. *Toxicol Pathol* **27**: 134–142.

Bolon B, Stolina M, King C, Middleton S, Gasser J, Zack D, and Feige U (2011) Rodent preclinical models for developing novel antiarthritic molecules: comparative biology and preferred methods for evaluating efficacy. *J Biomed Biotechnol* **2011**:569068.

Burke A, Smyth E, and Fitzgerald GA (2006) Analgesic-antipyretic agents, pharmacotherapy of gout, in *Goodman and Gilman. Pharmacological Bases of Therapeutics*, 11th ed, (Brunton LL, Lazo JS, and Parker KL eds) pp 671–715, McGraw Hill Company Incorporation, New York.

Caplazi P, Baca M, Barck K, Carano RA, DeVoss J, Lee WP, Bolon B, and Diehl L (2015) Mouse models of rheumatoid arthritis. *Vet Pathol* **52**:819–826.

Chatzidionysiou K, Emamikia S, Nam J, Ramiro S, Smolen J, van der Heijde D, Dougados M, Bijlsma J, Burmester G, Scholte M, et al. (2017) Efficacy of glucocorticoids, conventional and targeted synthetic disease-modifying antirheumatic drugs: a systematic literature review informing the 2016 update of the EULAR recommendations for the management of rheumatoid arthritis. *Ann Rheum Dis* **76**:1102–1107.

Cohen S, Zwillich SH, Chow V, Labadie RR, and Wilkinson B (2010) Co-administration of the JAK inhibitor CP-690,550 and methotrexate is well tolerated in patients with rheumatoid arthritis without need for dose adjustment. *Br J Clin Pharmacol* **69**:143–151.

Combe B, Landewe R, Daien CI, Hua C, Aletaha D, Álvaro-Gracia JM, Bakkers M, Brodin N, Burmester GR, Codreanu C, et al. (2017) 2016 update of the EULAR recommendations for the management of early arthritis. *Ann Rheum Dis* **76**: 948–959.

Gibaldi M and Perrier D (1982) *Pharmacokinetics*, 2nd ed, Marcel Dekker, New York.

Godfrey C, Sweeney K, Miller K, Hamilton R, and Kremer J (1998) The population pharmacokinetics of long-term methotrexate in rheumatoid arthritis. *Br J Clin Pharmacol* **46**:369–376.

Hegen M, Keith JC Jr, Collins M, and Nickerson-Nutter CL (2008) Utility of animal models for identification of potential therapeutics for rheumatoid arthritis. *Ann Rheum Dis* **67**:1505–1515.

Helleberg L (1981) Clinical pharmacokinetics of indomethacin. *Clin Pharmacokinet* **6**:245–258.

Kannan K, Ortmann RA, and Kimpel D (2005) Animal models of rheumatoid arthritis and their relevance to human disease. *Pathophysiology* **12**:167–181.

Keystone EC, Schiff MH, Kremer JM, Kafka S, Lovy M, DeVries T, and Burge DJ (2004) Once-weekly administration of 50 mg etanercept in patients with active rheumatoid arthritis: results of a multicenter, randomized, double-blind, placebo-controlled trial. *Arthritis Rheum* **50**:353–363.

Kollias G, Papadaki P, Apparailly F, Vervoordeldonk MJ, Holmdahl R, Baumans V, Desaintes C, Di Santo J, Distler J, Garside P, et al. (2011) Animal models for arthritis: innovative tools for prevention and treatment. *Ann Rheum Dis* **70**: 1357–1362.

Lee EB, Fleischmann R, Hall S, Wilkinson B, Bradley JD, Gruben D, Koncz T, Krishnaswami S, Wallenstein GV, Zang C, et al.; ORAL Start Investigators (2014) Tofacitinib versus methotrexate in rheumatoid arthritis. *N Engl J Med* **370**: 2377–2386.

Liu L, Di Paolo J, Barbosa J, Rong H, Reif K, and Wong H (2011) Antiarthritis effect of a novel Bruton's tyrosine kinase (BTK) inhibitor in rat collagen-induced arthritis and mechanism-based pharmacokinetic/pharmacodynamic modeling: relationships between inhibition of BTK phosphorylation and efficacy. *J Pharmacol Exp Ther* **338**:154–163.

Pearson CM (1956) Development of arthritis, periarthritis and periostitis in rats given adjuvants. *Proc Soc Exp Biol Med* **91**:95–101.

Ramiro S, Sepriano A, Chatzidionysiou K, Nam JL, Smolen JS, van der Heijde D, Dougados M, van Vollenhoven R, Bijlsma JW, Burmester GR, et al. (2017) Safety of synthetic and biological DMARDs: a systematic literature review informing the 2016 update of the EULAR recommendations for management of rheumatoid arthritis. *Ann Rheum Dis* **76**:1101–1136.

Saul PA and Korlipara K (1991) Acemetacin and indomethacin in the treatment of rheumatoid arthritis: a double-blind comparative study in general practice. *Curr Med Res Opin* **12**:332–341.

Schuck E, Bohnert T, Chakravarty A, Damian-Iordache V, Gibson C, Hsu CP, Heimbach T, Krishnatry AS, Liederer BM, Lin J, et al. (2015) Preclinical pharmacokinetic/pharmacodynamic modeling and simulation in the pharmaceutical industry: an IQ consortium survey examining the current landscape. *AAPS J* **17**: 462–473.

Strand V, Lee EB, Fleischmann R, Alten RE, Koncz T, Zwillich SH, Gruben D, Wilkinson B, Krishnaswami S, and Wallenstein G (2016) Tofacitinib versus methotrexate in rheumatoid arthritis: patient-reported outcomes from the randomised phase III ORAL start trial. *RMD Open* **2**:e000308.

Trentham DE, Townes AS, and Kang AH (1977) Autoimmunity to type II collagen an experimental model of arthritis. *J Exp Med* **146**:857–868.

Wong H, Bohnert T, Damian-Iordache V, Gibson C, Hsu CP, Krishnatry AS, Liederer BM, Lin J, Lu Q, Mettetal JT, et al. (2017) Translational pharmacokinetic-pharmacodynamic analysis in the pharmaceutical industry: an IQ consortium PK-PD discussion group perspective. *Drug Discov Today* **22**:1447–1459.

Wong H, Choo EF, Alicke B, Ding X, La H, McNamara E, Theil FP, Tibbitts J, Friedman LS, Hop CECA, et al. (2012a) Antitumor activity of targeted and cytotoxic agents in murine subcutaneous tumor models correlates with clinical response. *Clin Cancer Res* **18**:3846–3855.

Wong H, Vernillet L, Peterson A, Ware JA, Lee L, Martini JF, Yu P, Li C, Del Rosario G, Choo EF, et al. (2012b) Bridging the gap between preclinical and clinical studies using pharmacokinetic-pharmacodynamic modeling: an analysis of GDC-0973, a MEK inhibitor. *Clin Cancer Res* **18**:3090–3099.

Address correspondence to: Dr. Harvey Wong, Faculty of Pharmaceutical Sciences, The University of British Columbia, 2405 Wesbrook Mall, Vancouver, BC, Canada V6T 1Z3. E-mail: harvey.wong@ubc.ca